

Study on Ensemble-Based Forecast of Extremely Heavy Rainfalls in China: Experiments for July 2011 Cases

LIU Lin^{1,3} (刘琳), CHEN Jing^{2*} (陈静), CHENG Long³ (程龙), LIN Chunze¹ (林春泽),
and WU Zhipeng³ (吴志鹏)

¹ Hubei Key Laboratory for Heavy Rain Monitoring and Warning Research, Institute of Heavy Rain,
China Meteorological Administration, Wuhan 430074

² Numerical Weather Prediction Center, Beijing 100081

³ Chengdu University of Information Technology, Chengdu 610225

(Received August 1, 2012; in final form December 31, 2012)

ABSTRACT

According to the Anderson-Darling principle, a method for forecast of extremely heavy rainfall (abbreviated as extreme rainfall/precipitation) was developed based on the ensemble forecast data of the T213 global ensemble prediction system (EPS) of the China Meteorological Administration (CMA). Using the T213 forecast precipitation data during 2007–2010 and the observed rainfall data in June–August of 2001–2010, characteristics of the cumulative distribution functions (CDFs) of the observed and the T213 EPS forecast precipitation were analyzed. Accordingly, in the light of the continuous differences of the CDFs between model climate and EPS forecasts, a mathematical model of Extreme Precipitation Forecast Index (EPFI) was established and applied to forecast experiments of several extreme rainfall events in China during 17–31 July 2011. The results show that the EPFI has taken advantage of the tail information of the model climatic CDF and provided agreeable forecasts of extreme rainfalls. The EPFI based on the T213 EPS is useful for issuing early warnings of extreme rainfalls 3–7 days in advance. With extension of the forecast lead time, the EPFI becomes less skillful. The results also demonstrate that the rationality of the model climate CDF was of vital importance to the skill of EPFI.

Key words: extremely heavy precipitation, ensemble forecast, extreme precipitation forecast index, model climatic cumulative distribution function

Citation: Liu Lin, Chen Jing, Cheng Long, et al., 2013: Study on ensemble-based forecast of extremely heavy rainfalls in China: Experiments for July 2011 cases. *Acta Meteor. Sinica*, **27**(2), 170–185, doi: 10.1007/s13351-013-0203-y.

1. Introduction

The past decades have witnessed the great impacts of extreme weather and climate events on human society and the environment. There are a number of methods to define extreme events (Easterling et al., 2000). Beniston et al. (2007) pointed out that the extreme events can be divided into three types: (1) the events that have a relatively larger or smaller intensity; (2) the events that rarely take place; and (3) the events that lead to serious social losses. In the third and

fourth Intergovernmental Panel on Climate Change (IPCC) assessment reports (IPCC, 2001, 2007), the above definition (2) was adopted to identify extreme events, i.e., the small probability events that usually occur only 10% or even less of such weather phenomena in a particular place at a certain time. This definition avoids the large differences induced by the absolute intensity of an extreme event in different regions.

Extremely heavy precipitation (abbreviated as extreme precipitation or extreme rainfall hereafter) has been a subject of many studies. Most of these

Supported by the National Natural Science Foundation of China (41075035), National Science and Technology Support Program of China (2009BAC51B00), National Basic Research and Development (973) Program of China (2012CB417204), and China Meteorological Administration Special Public Welfare Research Fund (GYHY200906007).

*Corresponding author: chenj@cma.gov.cn.

Chinese version to be published

©The Chinese Meteorological Society and Springer-Verlag Berlin Heidelberg 2013

studies employed an extreme precipitation index to analyze the features and variations of the extreme events based on observations. Yamamoto and Sakurai (1999), Groisman et al. (1999), and Osborn et al. (2000) investigated the long-term variations of precipitation and heavy precipitation, and showed that there is an increasing trend in occurrence of extreme precipitation events. Yan and Yang (2000) noted that the drought in northern China reflects a significant reduction in trace precipitation events. Huang et al. (2003) detected that there is a continuous drought in North China and an increasing trend in summer monsoon precipitation over the Yangtze and Huaihe River basins since 1976. Zhai and Pan (2003), Qian and Lin (2005), and Zhang and Wei (2009) studied the variations of extreme precipitation in different areas in China, and obtained similar results. They found that the frequency of extreme precipitation events increased in Southwest, northern Northwest, and East China, but it decreased in North and Central China. Li et al. (2008) showed that summer precipitation in East China is mainly related to the intensity of rainstorms which produce more than 60% of the total precipitation. They also found that the amount and frequency of the rainfalls, the frequency of the extreme precipitation events, and the intensity of the rainstorms have increased in summer over the Yangtze River basin. Wang et al. (2008) used a regional coupled general circulation model (GCM) to simulate the extreme precipitation events in summer in China. Their results showed that the regional coupled GCM was able to simulate the spatial distribution of the mean threshold of the extreme precipitation. The study from Lu et al. (2009) showed that the initial moisture conditions had a great impact on the time when the maximum precipitation occurred.

As we know, the atmosphere is a chaotic system. Uncertainty of weather forecast is an inherent property of the chaotic system (Ye et al., 2006). Extreme precipitation is a small probability event that occurs with a great deal of uncertainty. Prediction of extreme precipitation is a difficult task. As a new method of probabilistic forecasting, ensemble forecasting provides a new prospect for small probability extreme events (Li and Chen, 2002; Chen et al.,

2005). Probability forecasting has been used in studies of extreme precipitation events for a long time. Steven and Jun (2001) used the short-range ensemble forecasting system of NCEP to simulate a snowstorm in North Carolina on 25 July 2000. They found that most ensemble members could successfully forecast this snowstorm. Sobash et al. (2011) indicated that the “neighborhood” (Theis et al., 2005) technique will be even more valuable in probabilistic forecasting of extreme events when implemented within a convection-allowing ensemble forecasting system.

So far, little such work has been done in China. Jiang et al. (2009) examined seven GCMs and five ensemble forecast models that are referred to in the fourth IPCC assessment. They pointed out that the GCMs were able to simulate the spatial distribution of the extreme precipitation index and to reflect its regional linear tendency in China. They also found that the skill of the ensemble forecast is better than that of the single model. Based on the Bayesian method, Chen et al. (2010) improved the heavy rainfall ensemble prediction by using climatological rainstorm observations from 147 stations in Sichuan. They showed that this method can eliminate the false prediction to some extent. By adopting four multi-model ensemble schemes to produce the probability density function (PDF) prediction of summer rainfalls over East China from 1960 to 2005, Li (2011) reported that the optimal ensemble scheme can well calibrate the original deterministic prediction, and the ensemble predictions are better or approximately equal to the climatological prediction.

Lalurette (2002) developed an extreme forecast index (EFI) based on the ECMWF ensemble prediction. The principle of the EFI is to compute the continuous probability differences of the cumulative distribution function (CDF) between the model climate and the ensemble prediction system. The results of Lalurette (2002) indicated that EFI can be used to well predict the extreme events even five days in advance. Lalurette (2003) revised the EFI formula by means of the Anderson and Darling (1952) theory and improved the sensitivity of EFI to extreme events. Ervin (2006) regenerated the CDF with ERA40 reanalysis and improved the EFI forecast skill.

Research on the ensemble-based forecast of extreme events is still at its preliminary stage in China. Xia and Chen (2012) evaluated the ensemble forecast method in predicting the extreme low temperature event in January 2008 with the T213 ensemble forecast product. They found that the EFI has a good ability to identify the extreme cold events 3–5 days in advance, and the forecast skill gradually decreased with the increase of the forecast lead time. Nonetheless, the application of EFI to predictions of other extreme events (e.g., extreme precipitation, extreme strong winds, etc.) remains unattended. It is known that precipitation is a non-continuous variable, which is different from temperature. Does the EFI still work for the prediction of extreme rainfalls?

In this paper, we propose a method for forecast of extreme rainfalls using the precipitation product from the China Meteorological Administration (CMA) T213 global ensemble prediction system (EPS). We will analyze the characteristics of the CDF derived from the T213 EPS forecast precipitation data in comparison with that from the observed precipitation data. After that, we will establish a mathematical model of the extreme precipitation forecast index (EPFI), and the skill of the index will be verified by simulations of several extreme rainfall events that happened in China in July 2011.

2. Data

In this paper, daily 24-h cumulative rainfall obser-

vations at 2412 stations in China during June–August of 2001–2011 were used (Fig. 1a). The data were provided by the National Meteorological Information Center of CMA. The precipitation product from the T213 EPS includes the data in July 2007 and the data in June–August of 2008–2011 at 24–168-h forecast lead times on $0.5625^\circ \times 0.5625^\circ$ grids (Fig. 1b).

Figure 1a shows the geographic location of the observation stations. Figure 1b gives the grid map of the T213 model over China. It can be seen that the stations are unevenly distributed. They are intensively distributed in the east and south of China but sparsely distributed in the northwest, especially in Xinjiang and the Tibetan Plateau. In this paper, the Cressman method (Chen and Shi, 2010) was used to interpolate the rainfall data at the 2412 stations onto the T213 grid points ($n = 3182$), as shown in Fig. 1b.

3. Comparison between the observed and the ensemble forecast extreme precipitation

Prior to studying the method for ensemble-based prediction of extreme rainfalls, we now compare the features in the observed rainfall and the T213 EPS forecast extreme precipitation. The differences in the geographic distribution of extreme precipitation and in the error distribution of the ensemble forecast extreme precipitation are examined, based on which a more reasonable prediction model and forecast index can be established for extreme rainfalls in China. The

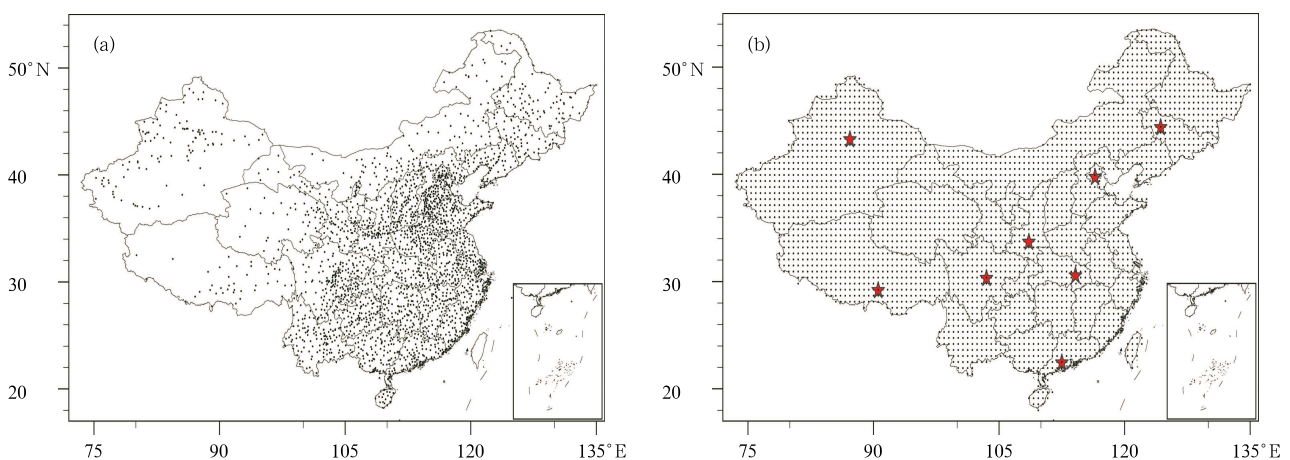


Fig. 1. Spatial distributions of (a) the 2412 rainfall observation stations and (b) the model grids. The stars in (b) denote grid points that are representative for the eight sub-regions under study.

Table 1. Geographic information on the eight sub-regions and their representative grid points

Grid number	Sub-region	Longitude	Latitude
1	Northeast China	124.31	44.44
2	Western Northwest China	87.19	43.31
3	Eastern Northwest China	108.56	33.75
4	North China	115.88	39.38
5	Mid-lower Yangtze River valley	114.19	30.38
6	Southwest China	103.50	30.38
7	South China	112.50	22.50
8	Tibetan Plateau	90.56	29.25

CDFs of the extreme rainfalls are different in different regions because of the topography in China. Thus, eight different climatic sub-regions of China are demarcated (Fig. 1b and Table 1) (Chen and Shao, 1991). For simplicity, we select a representative grid point in each sub-region, with its location denoted by a star in Fig. 1b.

3.1 Definition of extreme precipitation and characteristics of the ensemble forecast extreme precipitation

The extreme precipitation is defined by the percentile method (Zhai and Pan, 2003). First, the observed daily precipitation at each grid point during June–August of 2001–2010 is arranged in an ascending order. Then, the 10-yr mean 99th percentile of the precipitation observations is assigned as the threshold of the extreme precipitation, which only occurs when the daily precipitation exceeds the threshold.

The model precipitation serial is derived from the ensemble forecast product. It covers the period from June to August of 2008–2010. The length of this data serial is 4140, and the threshold is the 99th percentile of the model climatic precipitation.

The Γ distribution is used to fit the model precipitation distribution (Liu and Wu, 2005) according to the skewed probability distribution of the daily observed summer precipitation. Figure 2 shows the precipitation probability distribution of the ensemble forecast at the eight points at 24–168-h forecast lead times. It can be seen that the probability density distribution of the 24–168-h precipitation forecast at different grid points shows a consistent trend. But the probability density distribution for different effective forecast times is slightly different. Overall, the differ-

ences in the probability density distribution of different forecast lead times are obvious when precipitation amounts to 10–40 mm. The probability density distribution of 24 h is the largest. As the forecast lead time increases to 144 h, the probability density of the model climate precipitation gradually decreases. The probability density of 168-h forecast precipitation is improved when compared with the probability density of 144 h. The probability density of the precipitation greater than 40 mm gradually decreases and tends to approach zero when the forecast time increases. It is worth noticing that the precipitation probability density of the 168-h forecast precipitation is substantially constant. This means that the frequencies of heavy and moderate rains gradually decrease and the frequency of light rain increases when the forecast lead time increases. The probability density of 168-h forecast precipitation of different intensity scales tends to stabilize.

3.2 Comparison between the observed and the ensemble forecast precipitation

The observed and the ensemble forecast precipitation data during June–August of 2008–2010 are used to compare the characteristics of the observed and the model extreme precipitation. The spatial distributions of the observed and the model extreme precipitation are obtained according to the definition in Section 3.1. Figure 3a shows the observation and Figs. 3b–3d give the model results at 24–168-h forecast lead times, respectively.

It can be seen that the horizontal distribution of the forecast extreme precipitation is in general consistent with that of the observation. The precipitation gradually decreases from Southeast to Northwest

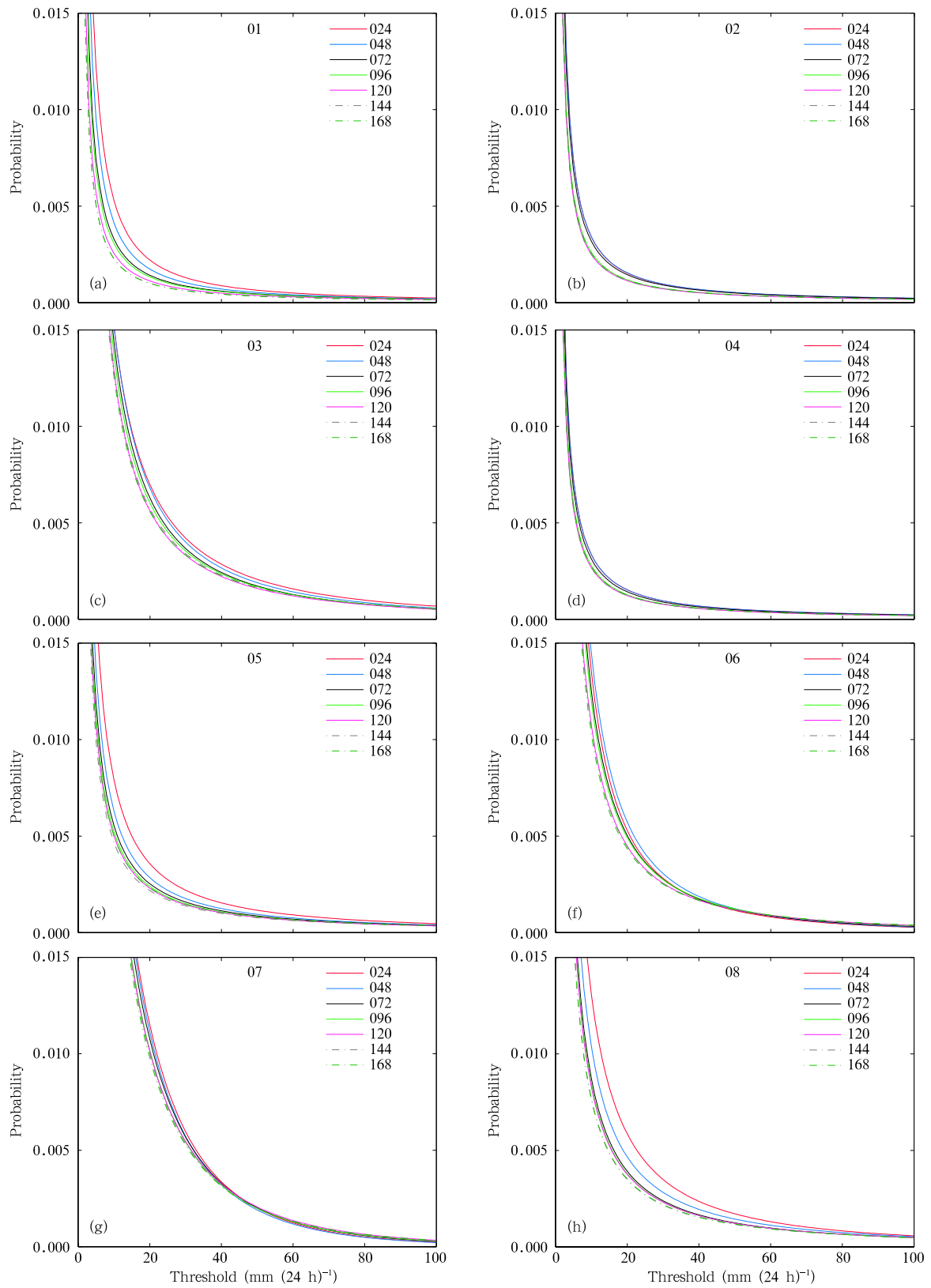


Fig. 2. Precipitation probability distribution of the ensemble forecast system at the representative grid points of the eight sub-regions (a–h).

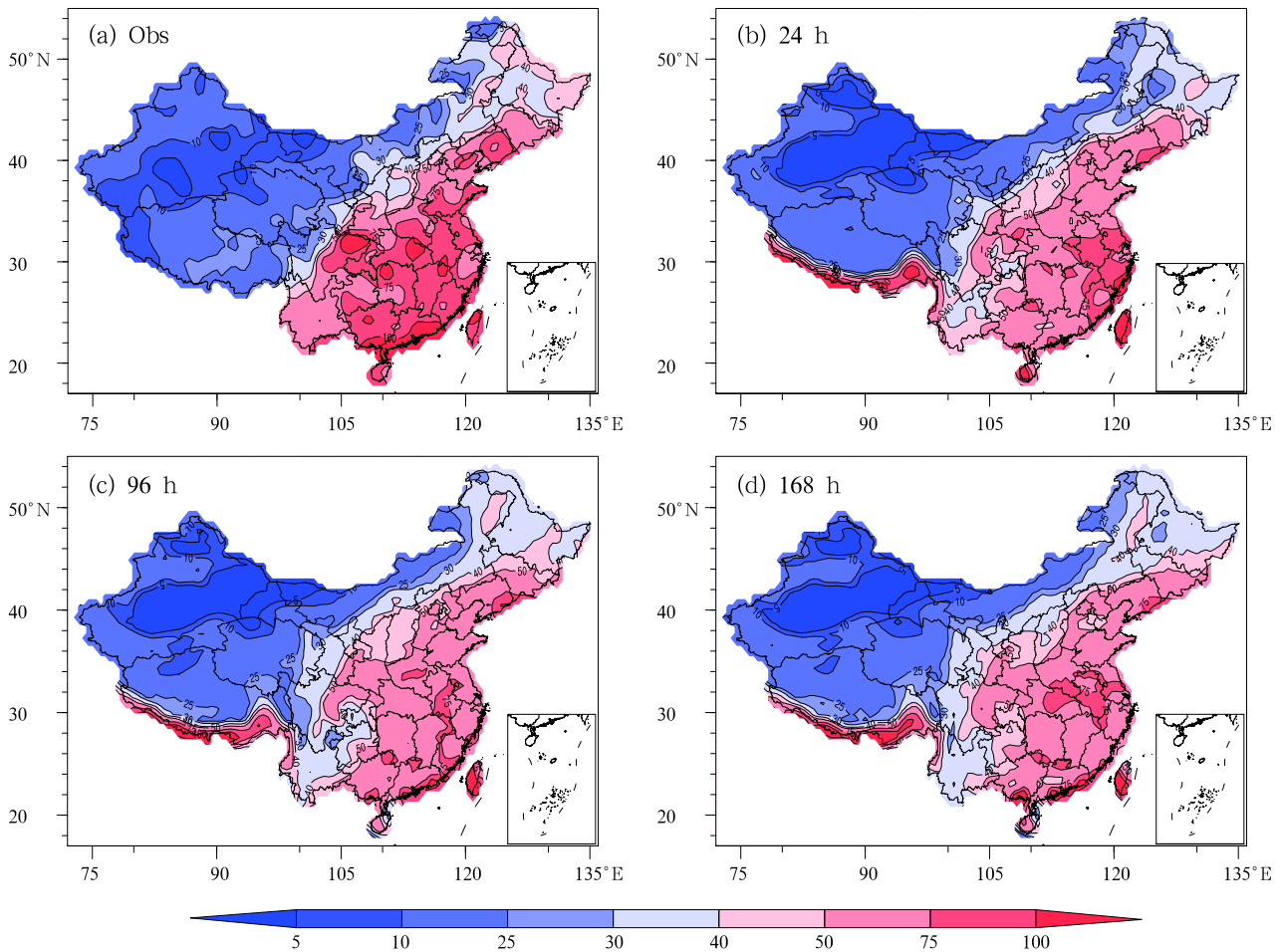


Fig. 3. Spatial distributions of (a) observed and (b) 24-, (c) 96-, and (d) 168-h ensemble forecast extreme precipitation.

China. The maximum rainfall centers in the model forecasts deviate from those in the observation. There are five centers in the observed extreme precipitation, located in the adjacent area of Sichuan and Shanxi, Hubei and Hunan, the Dabie Mountain, Guangdong, and other coastal areas. But the locations of the model forecast precipitation centers are different, with the maximum rainfall appearing in the southeast of the Tibetan Plateau and overestimated by model forecasts, and the maximum rainfall in the coastal areas in observation now near Jiangsu, Zhejiang, and Fujian provinces in the ensemble forecasts. The other large centers of the model extreme precipitation are in accordance with those of the observation. Figure 3 also shows that the model extreme precipitation is obviously less than the observed, especially in East China, and it decreases with the increase of the forecast lead

time.

4. Methodology of ensemble-based extreme rainfall forecast

4.1 Theory

The ensemble forecast of extreme rainfalls is based on the continuous differences of CDF between the historical model climate and the ensemble members, which could imply whether the extremes occur. We now take the CDFs of 48- and 96-h forecasts as well as the CDF of the model climate as examples to explain this theory. Figure 4 shows a schematic diagram of ensemble-based extreme precipitation forecast. In Fig. 4, solid lines represent the model climate CDF curves, dashed lines represent the CDFs of the ensemble forecasts; green lines are for 48-h and black

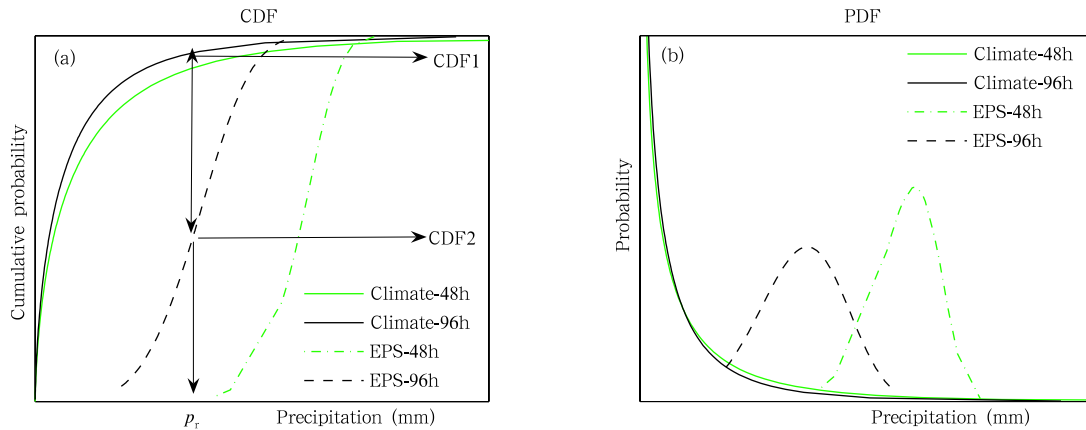


Fig. 4. Schematic diagrams of ensemble-based extreme precipitation forecast. (a) Vertical axis represents cumulative probability; lateral axis represents precipitation. Solid line represents the CDF curve of the model climate; dashed line represents the CDF curve of the ensemble forecasts (green line for 48 h and black line for 96 h). (b) Vertical axis represents probability density; lateral axis represents precipitation. Solid line represents the PDF curve of the model climate; dashed line represents the PDF curve of the ensemble forecasts (green line for 48 h and black line for 96 h).

lines for 96-h ensemble forecasts. Figure 4b shows the corresponding probability density distribution. The historical model climate at 48 and 96 h is separately collected by 48- and 96-h forecast precipitation of each T213 ensemble member in July of 2007–2010, and the serial length is 1860 (4 yr \times 31 days \times 15 ensemble members). The 48- and 96-h precipitation forecasts by the T213 EPS on 20 July 2011 are chosen as the ensemble forecast distribution serials, each of which is composed of 15 ensemble forecast members.

As seen in Fig. 4a, the model climate CDF at 96 h is CDF1, and the CDF of the ensemble forecasts is CDF2 when precipitation is P_r . The difference between CDF1 and CDF2 is greater than zero. This indicates that the ensemble forecast probability is greater than the model history when precipitation is greater than P_r . The area between the cumulative probability curve of the 96-h ensemble forecast and the model history is the continuous integration of the difference between the two curves within the 96-h forecast precipitation range. If the integration is greater than zero, the ensemble forecast precipitation is more than the model history. If the cumulative probability of the ensemble forecast precipitation tends to distribute at the tail (right side) of the model climatic CDF curve, the area increases. It can be seen from Fig. 4a that the area between the cumulative probability curve of the 48-h ensemble forecast and the model history is

larger than that of the 96-h ensemble forecast. Figure 4b gives the probability density at 48 and 96 h, corresponding to Fig. 4a. It can be found that the total amount of the 48-h ensemble forecast precipitation in the concentrated region is more than that of 96-h forecast precipitation, and the 48-h precipitation is heavier than the 96-h precipitation. Thus, the 48-h ensemble forecast has a better skill for predicting heavy rains than the 96-h ensemble forecast.

The above analysis shows that the continuous differences between the cumulative probability of the model history and the ensemble members can be used to measure the precipitation intensity. If the difference is positive, more precipitation and wet conditions may dominate, and vice versa.

4.2 Mathematical model of the extreme precipitation forecast index based on the Anderson-Darling test

Based on the theory of Anderson and Darling (1952), Lalaurette (2002) defined the EPFI formula:

$$\text{EPFI} = \frac{2}{\pi} \int_0^1 \frac{p - F_{f(p)}}{\sqrt{p(1-p)}} dp, \quad (1)$$

where p is the CDF of the historical model climate. If the climatic distribution is put in an ascending order, each percentile represents a probability threshold $f(p)$. In that way, $f(0)$ and $f(1)$ separately correspond

to the minimum and maximum of the climate serial, and so on. $F_{f(p)}$ is taken as the cumulative probability of the ensemble forecast. EPFI is the sum of the difference between the cumulative probability of the history and the ensemble forecast at each percentile. $\frac{1}{\sqrt{p(1-p)}}$ is the weight coefficient. If $p = 1/2$, the weight coefficient is the smallest. If $p = 0$ or 1 , the weight coefficient is the biggest. This could improve the EPFI sensitivity to the extreme events distributed at the tail of the cumulative probability curve. To some extent, it can make a prediction of the extreme event. Equation (2) below is a discrete form, where $p_i = i/100$ ($i = 0, 1, 2, \dots, 100$).

$$\text{EPFI} = \frac{2}{\pi} \sum_{i=0}^{100} \left(\frac{p_i - F_{f(p_i)}}{\sqrt{p_i(1-p_i)}} \times 0.01 \right). \quad (2)$$

It can be easily found from Eq. (1) that EPFI has some properties as follows: EPFI is a real number between -1 and 1 . If the results of all ensemble members are less than the minimum climatic probability ($F_{f(p_i)}$ is 1 for all P_i), EPFI is -1 . This means that the extreme drought may occur. If the results of all ensemble members are more than the minimum climatic probability ($F_{f(p_i)}$ is 0 for all P_i), EPFI is 1 . This implies that an extreme precipitation event may occur. The closer the EPFI is to $-1(+1)$, the greater probability of the extreme drought (precipitation) event may happen.

The CDF of the model climate is an important component of EPFI. In this paper, we adopt the model climate CDF of T213 ensemble forecast precipitation from 2007 to 2010 with the Lalaurette (2002) method. Xia and Chen (2012) found that the T213 model forecast has different errors for different forecast periods of validity. In the first section, it has been found that the ensemble forecast precipitation has different probability densities for different forecast lead times. The frequency of light rain increases with the increase of the forecast lead time. This paper selects daily precipitation of the T213 ensemble forecast in July from 2007 to 2010, and 7 model climate serials are generated at each grid point with the length of 1860. In the following, the climate CDF scheme will be referred to as T213-P1 in order to distinguish it from the scheme in Section 6.

The CDFs of 24–168-h ensemble forecasts are cal-

culated using the daily precipitation from T213 ensemble forecasts in July from 2007 to 2010. The length of these serials is 15. The EPFI is computed using Eq. (2). The derived EPFI could then provide the basis for determining the critical threshold of extreme precipitation in the next sub-section.

4.3 Method for determining the critical threshold of the EPFI

The above analysis indicates that extreme precipitation/rainfall may occur when EPFI is positive. But the forecasters need to know when they can release an alarm for extreme heavy rainfalls based on the EPFI. In this section, we focus on the method for determining the critical threshold of the EPFI. Extreme rainfalls can be seen as dichotomous (yes/no). We can find a certain approach to determine the critical threshold. If EPFI is greater than this threshold, the forecaster can make a warning of extreme rainfall occurrence. How to determine this critical threshold?

It is known that the Threat Score (TS) and Bias (BS) are two most commonly used indices in the assessment of precipitation forecast. Based on the contingency table of dimorphic distribution (Table 2) of a real extreme rainfall event and the EPFI forecast, the TS, BS, hit rate (HR), and false alarm rate (FAR) can be obtained by using Eqs. (3)–(6).

We design an S index for identifying the critical threshold of EPFI with consideration of the physical significance of the TS and BS. As seen in Eq. (7), the S index is proportional to the TS and inversely proportional to $|\text{BS}-1|$. The way of using S index to identify the critical threshold is to take 10 numbers of 0.1, 0.2, 0.3, \dots , and 1.0 as the reference threshold for releasing an alarm with the EPFI. The S indices of these 10 reference thresholds are calculated by Eq. (7). Figure 5 gives 4-yr averaged S indices of the 10 reference thresholds for 24–168-h forecasts. Then, the EPFI corresponding to the maximum S index is selected as the critical threshold for a certain forecast period of validity. The critical thresholds of the 24–168-h extreme precipitation forecast are shown in Table 3. It can be found that the critical threshold of EPFI gradually decreases from 0.8 to 0.5 while the forecast period of validity increases to 168 h.

Table 2. Contingency table of dimorphic distribution

		EPFI forecast	
		Yes	No
Observed	Yes	NA	NC
	No	NB	ND

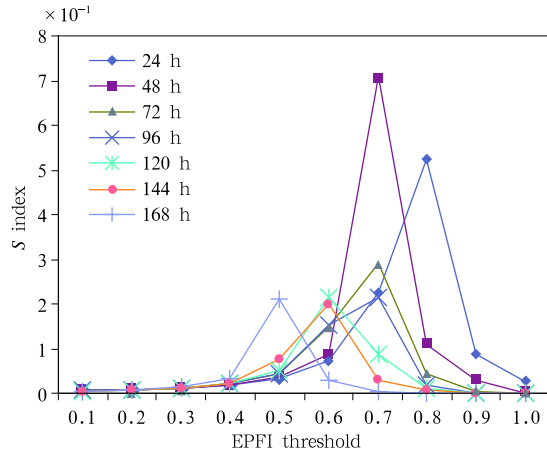


Fig. 5. Variations of the S index with different EPFI thresholds for 24–168-h forecast periods of validity.

$$TS = NA / (NA + NB + NC), \tag{3}$$

$$BS = (NA + NB) / (NA + NC), \tag{4}$$

$$HR = NA / (NA + NC), \tag{5}$$

$$FAR = NB / (NB + ND), \tag{6}$$

$$S = \begin{cases} \frac{TS}{|BS - 1|} & BS \leq 0.99 \text{ or } BS \geq 1.01, \\ TS \times 10^2 & 0.99 < BS < 1.01. \end{cases} \tag{7}$$

Table 3. The EPFI thresholds for 24–168-h forecast periods

Period of validity	Thresholds of EPFI
24 h	0.8
48 h	0.7
72 h	0.7
96 h	0.7
120 h	0.6
144 h	0.6
168 h	0.5

5. Experimental forecasts of extreme rainfalls in July 2011 with the CMA T213 ensemble forecast system

5.1 Experiments and verification during 15–31 July 2011

The EPFIs at each model grid point for seven forecast periods of validity are calculated by Eq. (2) based on the CDF of the ensemble forecasts and the

model climate during 15–31 July 2011. Table 4 shows the mean statistics of the extreme rainfall forecast. The TS gradually decreases with the increase of the forecast lead time. The TS of 24 h is the highest (0.15). The bias is proportional to the forecast period of validity, and the miss rate slightly increases with the increase of the forecast time while the hit rate decreases from 0.321 to 0.139. The false alarm rate increases to 0.044 when the forecast time reaches 168 h.

Relative Operating Characteristic (ROC) is an effective measure to evaluate the probabilistic forecast (Mason and Graham, 2002). It is obtained by plotting the hit rate and false alarm rate of different probabilities (EPFI can be divided into 10 grades) into one curve. If the curve is above the diagonal, the forecast skill is positive. The larger the area of ROC is, the better the forecast is. Figure 6 gives the mean ROC of the EPFI. The ROC is above the diagonal for forecast period of 24–168 h. It is closer to the diagonal with the increase of the forecast period. This indicates that all of the 24–168-h forecasts have positive forecast skills, which drop with the increase of the forecast period. The area of ROC (AROC) can be found in Table 4.

5.2 Extreme precipitation forecast on 24 July 2011

In this section, we assess the extreme precipita-

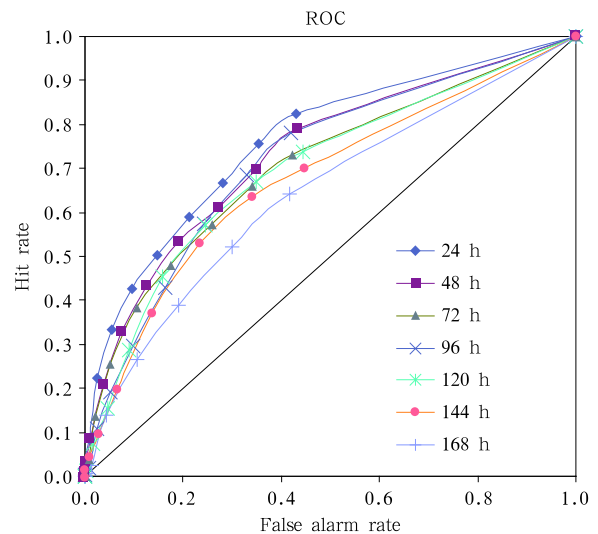


Fig. 6. The average Relative Operating Characteristic curve valid for the EPFI test. Each point of the curve corresponds to a different EPFI threshold.

Table 4. Statistics of the EPFI for extreme rainfalls during 15–31 July 2011

Score	24 h	48 h	72 h	96 h	120 h	144 h	168 h
TS	0.150	0.111	0.107	0.094	0.084	0.069	0.055
BS	1.168	1.156	1.723	1.573	1.298	1.911	1.589
HR	0.321	0.309	0.240	0.209	0.175	0.196	0.139
FAR	0.025	0.038	0.023	0.024	0.016	0.028	0.044
AROC	0.759	0.727	0.703	0.716	0.697	0.678	0.642

tion forecast on 24 July. The maximum precipitation appeared in Beijing, Tianjin, Liaoning and nearby. On that day, precipitation in some areas in Beijing was over 100 mm and the areal mean was 62 mm. The maximum cumulative precipitation occurred near the north of the Miyun Reservoir with 244 mm rainfall. Two deaths and one missing person were blamed on this extreme event. The precipitation in the east of Inner Mongolia and Shandong was more than 50 mm. According to the statistics, extreme rainfall occurred at a total of 76 grid points on 24 July, which accounts 2.39% of the total grids (Fig. 7). Most of these grid points are in the north of Inner Mongolia, Beijing, Hebei, Tianjin, central Shandong, the west and the south of Tibet.

Figure 8 shows distributions of 48–120-h forecast extreme rainfall. The start time of the forecasts is 0000 UTC 22 July, 0000 UTC 21 July, 0000 UTC 20 July, and 0000 UTC 19 July, respectively. The shaded areas are the regions where extreme rainfall appears judged by EPFI. Compared with the observation, the 48- and 72-h EPFIs correctly predicted the extreme events in the eastern Inner Mongolia, Beijing, Hebei, Tianjin, and western Tibet. But they missed the events in central Shandong and south of Tibet. The 72- and 96-h forecasts present similar results. The 120- and 144-h forecasts have also correctly predicted the events in the eastern Inner Mongolia, Beijing, Hebei, Tianjin, and western Tibet, but there are some false alarms which increase with extension of the forecast period in South China. The distribution of 24–96-h EPFI is very close to the observations (figures of the first few forecast times are omitted). Although the forecast skills of the 120-h or even longer lead times slightly decrease, the ensemble forecast approach still can predict the extremes in most regions at quite early lead times.

The above analyses show that the EPFI is indeed

able to make forecasts of extreme rainfalls even 3–7 days in advance, but the EPFI is unrealistically larger in South China. There are also some false alarms in the 120-h forecast in South China. The 48–120-h forecasts miss the extreme events in central Shandong. This may result from the fact that the model climate CDF only contains precipitation information in July. At that time, the rain belt jumps northward to North China, following the movement of the subtropical high, which leads to the increase of rainfall in North China and the decrease of rainfall in South China and the mid-lower reaches of Yangtze River. According to the climate CDF in South and Central China, the frequency of light rain increases. In North China, the occurrence probability of heavy rain increases. Thus, the EPFI is greater in South and Central China, and smaller in North China.

6. Impact of the model climatic CDF on the extreme precipitation forecast

It can be perceived from Eqs. (1) and (2) that the model climatic CDF has a great impact on the ensemble forecast of extreme precipitation. It is known

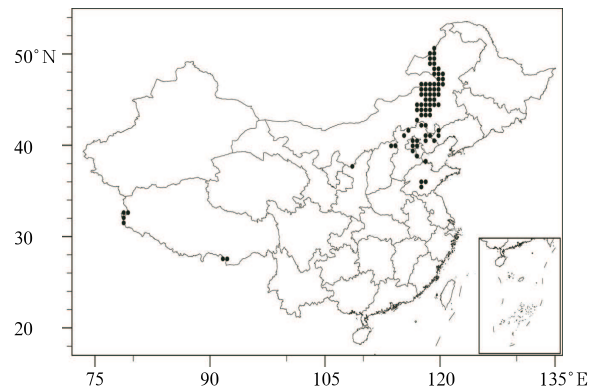


Fig. 7. Distribution of extreme precipitation grids on 24 July 2011.

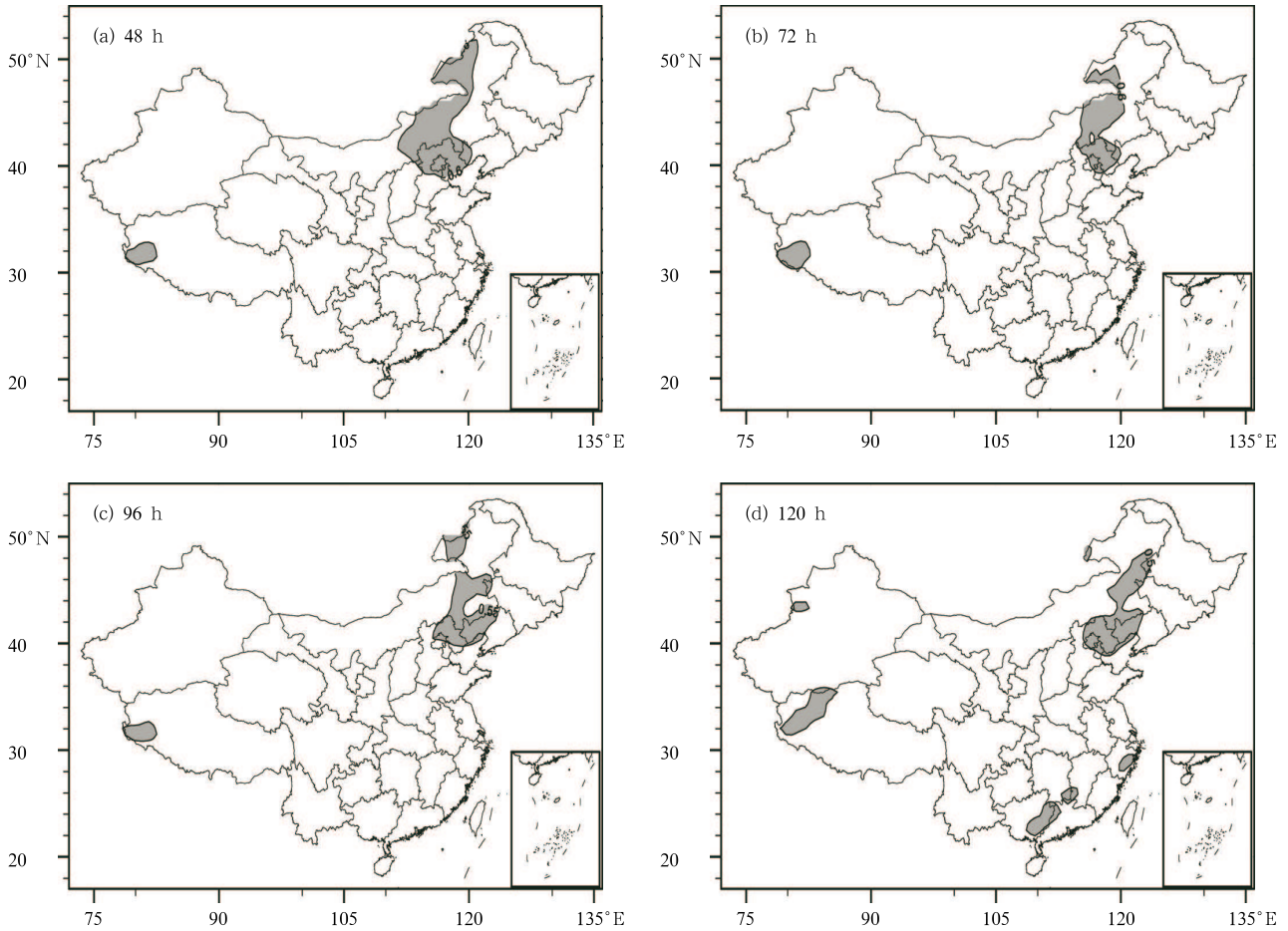


Fig. 8. Distributions of EPFI on 24 July 2011 at (a) 48-, (b) 72-, (c) 96-, and (d) 120-h forecast lead times.

that the rainy season in China falls mainly in June–August. The available historical model data in China cover a shorter time period than the ECMWF data. Accordingly, we compile a second set of model climate data. Daily precipitation forecast product from the T213 EPS at each grid point in China during June–August of 2008–2010 is selected. Seven independent model climate series (24–168 h) are generated at each grid point with a length of 4140 ($n = 3 \text{ yr} \times 92 \text{ days} \times 15 \text{ members}$), which is referred to as T213-P2 in the following.

Comparison between the CDFs of the two model climate datasets, i.e., T213-P2 and T213-P1, for 72-h forecast (the results of other forecast times are similar) in South China, North China, and the mid-lower reaches of Yangtze River is displayed in Fig. 9. The frequencies of light to moderate rains in North China

increase and the CDF curve is closer to y -axis. In South China and the mid-lower reaches of Yangtze River, the frequencies of moderate and heavy rains increase and the CDF curve is closer to x -axis. This trend is more obvious in South China. These results suggest that light rains occur more often in North China and moderate to heavy rains happen less frequently in central and South China based on T213-P2.

Figure 10 compares the EPFI maps from the two climate datasets T213-P1 and T213-P2 at 48 and 120 h, respectively. We can see that for 48-h forecasts, T213-P1 scheme missed the extreme precipitation in central Shandong while T213-P2 successfully captured it and set the alarm. For 120-h forecasts, the false alarm from T212-P1 appeared in a larger area in South China while the false alarm from T213-P2 decreased obviously in this area, suggesting an improved result

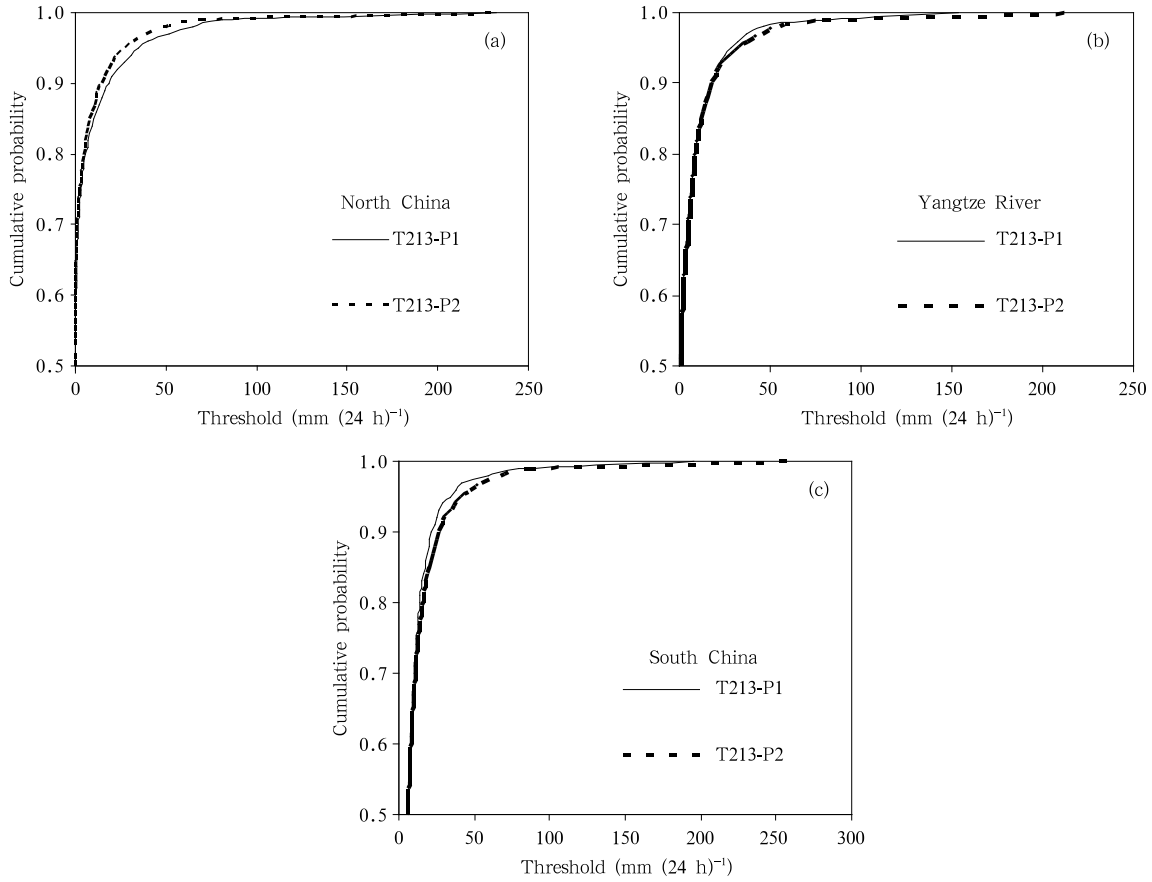


Fig. 9. Cumulative probability curves of the 72-h model climate precipitation datasets T213-P1 (solid) and T213-P2 (dashed) for (a) North China, (b) mid-lower reaches of Yangtze River, and (c) South China.

by using T213-P2. The other experiments produced similar results. Overall, T213-P2 reduces the misses in North China due to smaller EPFI, and also reduces the false alarms in South China.

The statistical results from comparisons of the two model climate datasets are given in Fig. 11. Both the TS and HR based on T213-P2 are higher than those based on T213-P1. The AROC of T213-P2 is also higher than T213-P1 (Table 5). However, the false alarm rate and the bias of T213-P2 are slightly higher than T213-P1, which means that although the hit rate of T213-P2 dwarfs that of T213-P1, its false alarm rate is defeated by that of T213-P1. Overall, the T213-P2 climate is better than the T213-P1.

Comparisons of the climatic CDF between the two model climate datasets show that T213-P2 has an improved EPFI forecast skill than T213-P1. T213-P2 has a higher probability to predict the extremes (although

it also has a higher false alarm rate). This may be because the raining season in China covers three continuous months (June–August); T213-P2 uses three-month data and thus contains more precipitation information than T213-P1 does, which uses only one-month data. It is therefore inferred that the model climatic CDF should contain as much objective precipitation information as possible.

7. Summary

Extremely heavy precipitation (abbreviated as extreme precipitation/rainfall throughout the text) is a small probability event that occurs with a great deal of uncertainty. It is very difficult for its accurate prediction. In this study, the differences between the observed and model forecast precipitation CDFs are analyzed with consideration of characteristics of the

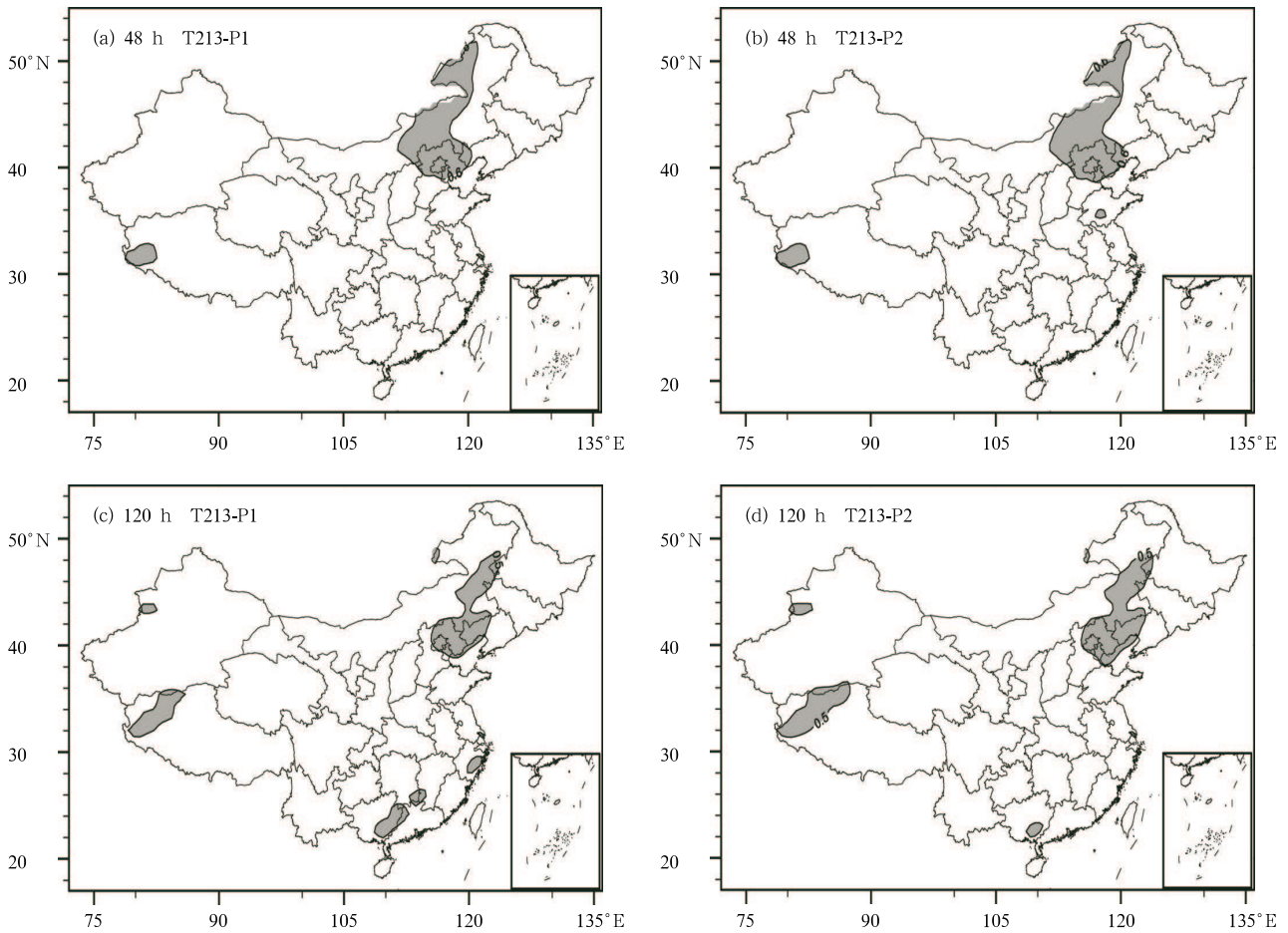


Fig. 10. EPFI maps derived from the two model climate precipitation datasets T213-P1 (a, c) and T213-P2 (b, d) on 24 July 2011 for 48- (a, b) and 120-h (c, d) forecasts.

Table 5. AROC of the two model climates of precipitation

AROC	24 h	48 h	72 h	96 h	120 h	144 h	168 h
T213-P1	0.759	0.727	0.703	0.716	0.697	0.678	0.642
T213-P2	0.762	0.724	0.711	0.731	0.710	0.696	0.661

T213 ensemble forecast precipitation. According to the Anderson-Darling test, an EPFI is established on the basis of the T213 ensemble forecast. The impact of the historical model CDF on the EPFI is examined through comparisons between experimental results on the extreme precipitation events that occurred in July 2011. Preliminary results are summarized as follows.

(1) Precipitation forecasts from the T213 ensemble prediction system show that the differences in the probability density distribution for different forecast lead times are obvious when the forecast precipitation is between 10 and 40 mm. Precipitation density de-

creases with the growth of the forecast time. When forecast rainfall is over 40 mm, the precipitation probability density is close to zero for different forecast times. When forecast precipitation is less than 10 mm, the precipitation probability increases. For precipitation events of all intensity levels, the precipitation probability begins to stabilize after the forecast time reaches 168 h.

(2) Comparisons between the observed and the model forecast precipitation show that the horizontal pattern of the model precipitation is close to the observation, but the model precipitation is less in mag-

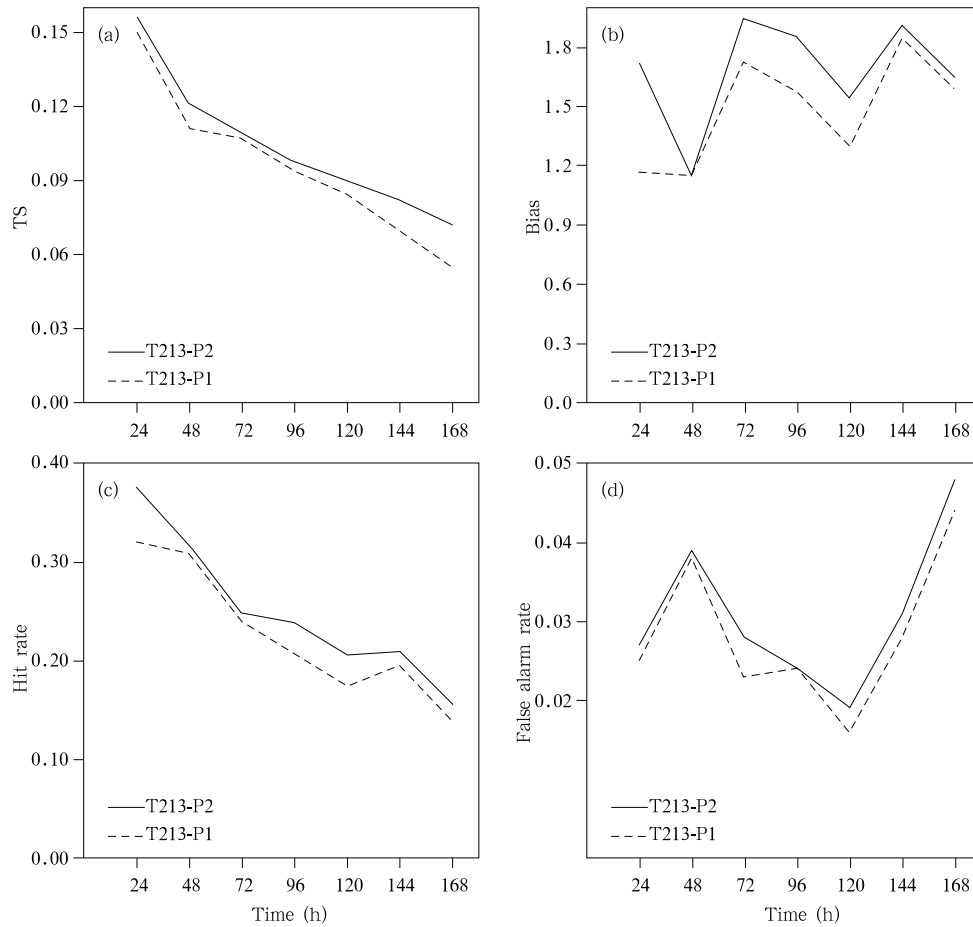


Fig. 11. Average test results of the two model climates of precipitation.

nitude than the observation. Besides, extreme precipitation decreases with the growth of the forecast time. There are some differences in the center location of the extreme rainfalls. The observed centers are in Guangdong Province and nearby areas whereas the model centers are near Jiangsu, Zhejiang, and Fujian provinces. Over the Tibetan Plateau, there is a fake center of extreme rainfall.

(3) The extreme precipitation forecast index (EPFI) has taken full advantage of the tail information of the CDF curve of ensemble forecasts. The results show that EPFI has a good ability to identify extreme precipitation, which enables an alarm to be set 3–7 days ahead of the extreme event. The EPFI forecast skill decreases with the increase of the forecast time.

(4) By comparing the CDF of two model climate datasets, we find that the forecast skill of the CDF

that contains historical model precipitation information from June to August is better than the CDF that contains only the July precipitation information. This may be associated with the actual length of the three-month rainy season of China. Thus, it is better for the model climatic CDF to include objective precipitation information as much as possible.

It should be pointed out that in this paper, we only obtained 5-yr data of the T213 ensemble forecast. How to take advantage of the existing data to generate a better model climatic CDF in order to improve the forecast skill of the EPFI on the extreme rainfalls needs to be further studied.

REFERENCES

- Anderson, T., and D. Darling, 1952: Asymptotic theory of certain goodness of fit criteria based on stochastic

- processes. *Annals of Mathematical Statistics*, **23**, 193–212.
- Beniston, M., D. B. Stephenson, O. B. Christensen, et al., 2007: Future extreme events in European climate: An exploration of regional climate model projections. *Climatic Change*, **81**(Suppl. 1), 71–95.
- Chen Fei and Shi Ping, 2010: Assimilation of hydrographic data in the northern South China Sea based on the Cressman objective analysis. *Journal of Tropical Oceanography*, **29**(4), 1–7. (in Chinese)
- Chen Longxun and Shao Yongning, 1991: Preliminary analysis of climatic change during the last 39 years in China. *J. Appl. Meteor. Sci.*, **2**(2), 164–174. (in Chinese)
- Chen Jing, Xue Jishan, and Yan Hong, 2005: A new initial perturbation method of ensemble mesoscale heavy rain prediction. *Chinese J. Atmos. Sci.*, **29**(5), 717–726. (in Chinese)
- Chen Zhaoping, Feng Hanzhong, and Chen Jing, 2010: Application of Sichuan heavy rainfall ensemble prediction probability products based on Bayesian method. *Meteor. Mon.*, **36**(5), 22–39. (in Chinese)
- Easterling, D. R., G. A. Meehl, C. Parmesan, et al., 2000: Climate extremes: Observations, modeling, and impacts. *Science*, **289**(5487), 2068–2074.
- Ervin, Z., 2006: Recent developments in extreme weather forecasting. ECMWF Newsletter No. 107–Spring, 8–17.
- Groisman, P. Y., T. R. Karl, D. R. Easterling, et al., 1999: Changes in the probability of heavy precipitation: Important indicators of climatic change. *Climatic Change*, **42**, 243–283.
- Huang Ronghui, Chen Jilong, Zhou Liantong, et al., 2003: Studies on the relationship between the severe climatic disasters in China and the East Asian climate system. *Chinese J. Atmos. Sci.*, **27**(4), 770–788. (in Chinese)
- IPCC, 2001: *Climate Change 2001: The Science of Climate Change*. Contribution of Working Group I to the Third Assessment Report of the Intergovernmental Panel on Climate Change. Houghton, J. T., Y. Ding, D. J. Griggs, et al., Eds., Cambridge University Press, Cambridge, United Kingdom and New York, NY, USA, 881 pp.
- , 2007: *Climate Change 2007: The Physical Science Basis*. Contribution of Working Group I to the Fourth Assessment Report of the Intergovernmental Panel on Climate Change. Solomon, S., D. Qin, M. Manning, et al., Eds., Cambridge University Press, Cambridge, United Kingdom and New York, NY, USA, 996 pp.
- Jiang Zhihong, Chen Weiling, Song Jie, et al., 2009: Projection and evaluation of the precipitation extreme indices over China based on seven IPCC AR4 coupled climate models. *Chinese J. Atmos. Sci.*, **33**(1), 109–120. (in Chinese)
- Lalurette, F., 2002: Early detection of abnormal weather conditions using a probabilistic extreme forecast index. *Quart. J. Roy. Meteor. Soc.*, **129**, 3037–3057.
- , 2003: Two proposals to enhance the EFI response near the tails of the climate distribution. http://www.ecmwf.int/products/forecasts/efi_guide.pdf, 1–8.
- Li Fang, 2011: Probabilistic seasonal prediction of summer rainfall over East China based on multi-model ensemble schemes. *Acta Meteor. Sinica*, **25**(3), 283–292, doi: 10.1007/s13351-011-0304-4.
- Li Hongmei, Zhou Tianjun, and Yu Rucong, 2008: Analysis of July–August daily precipitation characteristics variation in eastern China during 1958–2000. *Chinese J. Atmos. Sci.*, **32**(2), 358–370. (in Chinese)
- Li Zechun and Chen Dehui, 2002: The development and application of the operational ensemble prediction system at National Meteorological Center. *J. Appl. Meteor. Sci.*, **13**(1), 1–15. (in Chinese)
- Liu Xuehua and Wu Hongbao, 2005: Probability distribution of summer daily precipitation in China. *Trans. Atmos. Sci.*, **29**(2), 173–180. (in Chinese)
- Lu Ping, Yu Rucong, and Zhou Tianjun, 2009: Numerical simulation on the sensitivity of heavy rainfall over the western Sichuan basin to initial water vapor condition. *Chinese J. Atmos. Sci.*, **33**(2), 241–250. (in Chinese)
- Mason, S. J., and N. E. Graham, 2002: Areas beneath the relative operating characteristic (ROC) and relative operating level (ROL) curves: Statistical significance and interpretation. *Quart. J. Roy. Meteor. Soc.*, **128**, 2145–2166.
- Osborn, T. J., M. Hnhne, P. D. Jones, et al., 2000: Observed trends in the daily intensity of United Kingdom precipitation. *Int. J. Climatol.*, **20**, 347–364.
- Qian, W., and X. Lin, 2005: Regional trends in recent precipitation indices in China. *Meteor. Atmos. Phys.*, **90**(2), 193–207, doi: 10.1007/s00703-004-0101-z.

- Steven, T. M., and D. Jun, 2001: Application of the NCEP/EMC short range ensemble forecast system (SREF) to predicting extreme precipitation events. the 81st AMS Annual Meeting, Amer. Meteor. Soc., Albuquerque, NM, July, P1.25, 64–70.
- Sobash, R. A., et al., 2011: Probabilistic forecast guidance for severe thunderstorms based on the identification of extreme phenomena in convection-allowing model forecasts. *Wea. Forecasting*, **5**(26), 714–728.
- Theis, S. E., A. Hense, and U. Damrath, 2005: Probabilistic precipitation forecasts from a deterministic model: A pragmatic approach. *Meteor. Appl.*, **12**, 257–268.
- Wang Zhifu, et al., 2008: Analysis of numerical simulation on extreme precipitation in China using a coupled regional ocean-atmosphere model. *Plateau Meteor.*, **1**(2), 37–50. (in Chinese)
- Xia Fan and Chen Jing, 2012: The research of extreme forecast index based on the T213 ensemble forecast and the experiment in predicting temperature. *Meteor. Mon.*, **8**(12), 1513–1522. (in Chinese)
- Yamamoto, R., and Y. Sakurai, 1999: Long term intensification of extremely heavy rainfall intensity in recent 100 years. *World Resour. Rev.*, **11**, 271–281.
- Yan Zhongwei and Yang Chi, 2000: Geographic patterns of extreme climate changes in China during 1951–1997. *Climatic Environ. Res.*, **5**(3), 267–272. (in Chinese)
- Ye Duzheng, Yan Zhongwei, et al., 2006: A discussion of future system of weather and climate prediction. *Meteor. Mon.*, **32**(4), 3–8. (in Chinese)
- Zhai Panmao and Pan Xiaohua, 2003: Change in extreme temperature and precipitation over northern China during the second half of the 20th century. *Acta Geographica Sinica*, **58**(Suppl.), 1–10. (in Chinese)
- Zhang Ting and Wei Fengying, 2009: Probability distribution of precipitation extremes during raining seasons in South China. *Acta Meteor. Sinica*, **67**(3), 442–451. (in Chinese)